PLANT SCIENCE TODAY
Vol 13(1): 1-12
https://doi.org/10.14719/pst.12024

eISSN 2348-1900

RESEARCH ARTICLE

Integrating geostatistics and pollution indices to delineate chromium contamination hotspots and risk zones in an industrial landscape

Pandiya Kumar D[1], Jagadeeswaran Ramasamy[1*], Sellaperumal Pazhanivelan[2], Kumaraperumal Ramalingam[1], Prabu Padanillay Chidambaram[2] & R Pangayarselvi[3]

[1]Department of Remote Sensing and Geographic Information System, Tamil Nadu Agricultural University, Coimbatore 641 003, Tamil Nadu, India
[2]Centre for Water and Geospatial Studies, Tamil Nadu Agricultural University, Coimbatore 641 003, Tamil Nadu, India
[3]Department of Physical Sciences & Information Technology, Agricultural Engineering College and Research Institute, Tamil Nadu Agricultural University, Coimbatore 641 003, Tamil Nadu, India

*Correspondence email - jagawaran@tnau.ac.in

Received: 27 September 2025; Accepted: 05 November 2025; Available online: Version 1.0: 05 March 2026; Version 2.0: 19 March 2026

Cite this article: Pandiya Kumar D, Jagadeeswaran R, Pazhanivelan S, Kumaraperumal R, Prabu PC, Pangayarselvi R. Integrating geostatistics and pollution indices to delineate chromium contamination hotspots and risk zones in an industrial landscape. Plant Science Today. 2026; 13(1): 1-12. https://doi.org/10.14719/pst.12024

Abstract

Chromium (Cr) contamination in soils poses a major ecological and human health concern in industrial landscapes, particularly in tannery clusters. In this study, geostatistical methods and pollution indices were integrated to delineate Cr contamination hotspots and ecological risk zones in the Walaja block, Tamil Nadu, India. Sixty-eight surface soil samples were collected in September, 2024 and analysed for physicochemical properties and total Cr concentrations using standard protocols. The contamination factor (CF), geo-accumulation index (Igeo) and ecological risk index (Er) were computed. Spatial interpolation was performed using inverse distance weighting (IDW) and hotspots were identified with the Getis–Ord Gi* statistic. Soil Cr concentrations ranged from 129 to 2625 mg/kg (mean ≈ 601 mg/kg), which is over 27 times the natural background level. Contamination factor (CF) and Igeo values indicated severe to extreme contamination in the northwestern industrial corridor, whereas Er values were mostly in the low-to-moderate risk category due to Cr's relatively low toxicity factor. Spatial analysis confirmed statistically significant Cr hotspots in tannery zones and cold spots in agricultural areas. Integrated risk zonation classified approximately 20 % of the study area as high risk, 35-40 % as moderate risk and 40-45 % as low risk. These findings indicate that the high-risk areas coincide with tannery belts, underscoring the urgent need for soil remediation and stricter land-use regulation. The combined geostatistical-index approach provides a robust tool for policymakers to prioritize monitoring and mitigation efforts in industrial regions.

Keywords: chromium contamination; geostatistics; hotspot analysis; pollution indices; risk zonation; soil pollution

Introduction

Soil serves as the foundation of terrestrial life, supporting nearly 95 % of global food production and providing essential ecosystem services that regulate nutrient cycling, water filtration and carbon sequestration (1). However, soil resources are increasingly stressed: by 2050, food production must rise by 35–56 % to meet demand intensifying pressure on land. The Food and Agriculture Organization (FAO) warns that up to 90 % of soils could be degraded by 2050 due to erosion, intensive farming and industrial pollution (2). In this context, heavy metal contamination is a pervasive threat to soil health. Toxic elements such as arsenic (As), cadmium (Cd), nickel (Ni) and chromium (Cr) persist in soils, reducing fertility and contaminating crops and water (3, 4). Recent global assessments indicate that 14-17 % of croplands exceed safe thresholds for metal pollution, exposing roughly one billion people to elevated ecological and human health risks (2). Therefore, mapping the spatial distribution of heavy metals is critical for assessing environmental risk and guiding remediation efforts for sustainable land management (4).

Among heavy metals, Cr is of special concern in industrial regions. Chromium occurs naturally in soils, but human activities have greatly increased its environmental load. In soil environments, Cr typically exists as trivalent Cr (III) and hexavalent Cr (VI) (3). Numerous industrial processes contribute to Cr release into the environment, including metallurgy, electroplating, pigment and dye manufacturing, wood preservation and especially leather tanning (3, 5). In leather tanning, for example, large quantities of Cr (III) sulphate are applied to hides and untreated effluent can deposit thousands of mg/kg of chromium into adjacent soils. In soils, Cr (III) strongly binds to organic matter and is relatively immobile, whereas Cr (VI) is highly water-soluble and mobile. Notably, Cr (VI) is much more hazardous: it penetrates biological membranes easily and generates reactive oxygen species. Hexavalent chromium (Cr^{6+}) is classified as a Group 1 human carcinogen and has been linked to severe health effects, including lung cancer (6). In plants and soil organisms, excessive Cr causes phytotoxicity, with symptoms including stunted root and shoot growth, chlorosis, necrosis and suppressed biomass. Because chromium is non-biodegradable,

contaminated soils remain long-term sources of exposure and risk even after emissions cease (3).

Several recent studies have highlighted the severity of chromium contamination in industrial landscapes using geostatistics and pollution indices. In the Peenya Industrial Area of Bengaluru, soil Cr contamination was evaluated using indices such as the contamination factor (CF), enrichment factor (EF), geo-accumulation index (Igeo) and metal pollution index (MPI), revealing high subsurface Cr levels and elevated carcinogenic risks for children (7). At the Savar Tannery Estate in Bangladesh, sediment analyses reported Cr concentrations up to 748 mg/kg, with CF, Igeo and pollution load index (PLI) values indicating severe pollution hotspots near effluent discharge points (8). In Ranipet, Tamil Nadu, the integration of groundwater Cr (chromium) data with the DRASTIC vulnerability index identified extensive high-risk zones linked to tannery effluent contamination (9). These studies demonstrate the effectiveness of combining geostatistical and index-based approaches for understanding Cr contamination, but most of them either focus on water or sediment systems and lack an integrated soil risk-zonation framework.

The Walaja block of Tamil Nadu, India, serves as relevant case study. This region includes the Walajapet Taluk in Ranipet district, a major leather tanning and industrial cluster (10). Hundreds of tanneries and leather goods factories operate here, and their effluents contain high levels of chromium. Previous studies have documented severe Cr contamination in soils from this region, with more than 80% of agricultural soils surrounding the Walajapet tanneries exceeding the 200 mg/kg safety guideline for Cr. (11) Similarly, chromium concentrations as high as 2459 mg/kg have been reported in soils from the same area (10). These findings demonstrate that tannery discharges have heavily polluted local soils, but they do not show how contamination is distributed across the wider Walaja landscape. In particular, the locations of statistically significant Cr hotspots and the spatial gradation of ecological risk have not been mapped.

Geostatistical methods (e.g., semivariograms and kriging) can reveal spatial patterns and clusters of soil contaminants (4), while geochemical indices (e.g., contamination factor, geo-accumulation index, ecological risk index (Er)) provide quantitative measures of pollution severity (5). By integrating these tools, one can produce a Cr contamination and risk-zonation map to prioritize areas for action. In this study, an integrated approach is applied to Walaja block: soil Cr concentrations are mapped and interpolated spatially, standard pollution and risk indices are computed and both are used to identify critical hotspots. Correlations between soil Cr levels and soil physicochemical properties (pH, EC (electrical conductivity), SOC (soil organic carbon)) are also examined to infer potential contamination sources.

The objectives of this study are following: i) to determine the concentration and spatial distribution of Cr in the soils of Walaja block, Tamil Nadu; ii) to infer potential Cr sources by examining correlations with soil physicochemical properties; iii) to assess Cr contamination levels and associated ecological risk using geochemical indices; iv) to identify statistically significant spatial hotspots of Cr accumulation through geostatistical analysis; and v) to develop an integrated Cr risk-zonation map to prioritize areas for remediation.

Materials and Methods

Study area description

Walajapet (Walaja) block is located in Ranipet district, Tamil Nadu (formerly part of Vellore until 2019), between 13°–14°N and ≈78°E. The region has a semi-arid tropical climate, with very hot summers (mean maximum ≈ 32.5 °C) and mild winters (minimum ≈ 22.1 °C). Annual rainfall is about 1,000 mm, occurring mostly during the northeast monsoon (12). The soils are predominantly red, non-calcareous sandy loams derived from gneissic parent material. They are generally low in organic carbon and moderately well-drained (13). The soil reaction ranges from slightly acidic to moderately alkaline (range: 6-8), while EC values are low (<1 dS m^{-1}) and SOC content is very low. Land use is dominated by agriculture (e.g., paddy, sugarcane, groundnut, pulses, banana), with peri-urban settlements and industrial estates interspersed. The Palar River flows through the district and has historically provided irrigation water, although its baseflow has now greatly reduced (14).

Walajapet and neighbouring Ranipet together form one of South India's major leather industry clusters, hosting over 100 tanneries and allied industries (15). Effluent disposal - particularly Cr-rich tanning waste - has been identified as a major source of local soil and groundwater contamination (10, 11). The study area and soil sampling locations are illustrated in Fig. 1.

Soil sampling and laboratory analysis

Sixty-eight surface soil samples (0–30 cm depth) were collected in September 2024 across agricultural and peri-industrial areas of Walajapet block. Sites were selected by random accessibility sampling to represent different land uses. Approximately 1 kg of soil was collected at each site using a stainless-steel auger, placed in clean polyethylene bags, labelled and transported to the laboratory. Samples were air-dried and sieved to 2 mm (16).

Soil pH and EC were measured in a 1:2.5 soil-to-water suspension using a Labman 5-point benchtop pH meter and a Labman LMCM20H Conductivity/TDS meter. The pH meter was calibrated using standard buffer solutions of pH 4.0, 7.0 and 9.2, while the EC meter was calibrated with a 0.01 M KCl standard solution (1413 µS/cm at 25 °C) prior to measurement (17, 18). Soil organic carbon (SOC) was determined by the Walkley–Black wet oxidation method (19). Total chromium concentration was measured by inductively coupled plasma–optical emission spectrometry (ICP-OES; PerkinElmer Avio) after acid digestion using US EPA Method 3051a (20), which involves sequential digestion with HNO_3, H_2O_2 and HCl under reflux.

Pollution and ecological risk assessment

Chromium contamination and ecological risk were assessed using standard geochemical indices. The CF, Igeo and Er were determined to assess the level and potential risk of Cr contamination in the soil. The CF was calculated as the ratio of the measured Cr concentration to its background concentration. The CF, Igeo and Er were computed following the standard formulations and toxic-response factors as given in Table 1. A global average background value of 100 mg/kg for Cr in soils was adopted (25), consistent with values used in Indian studies (10).

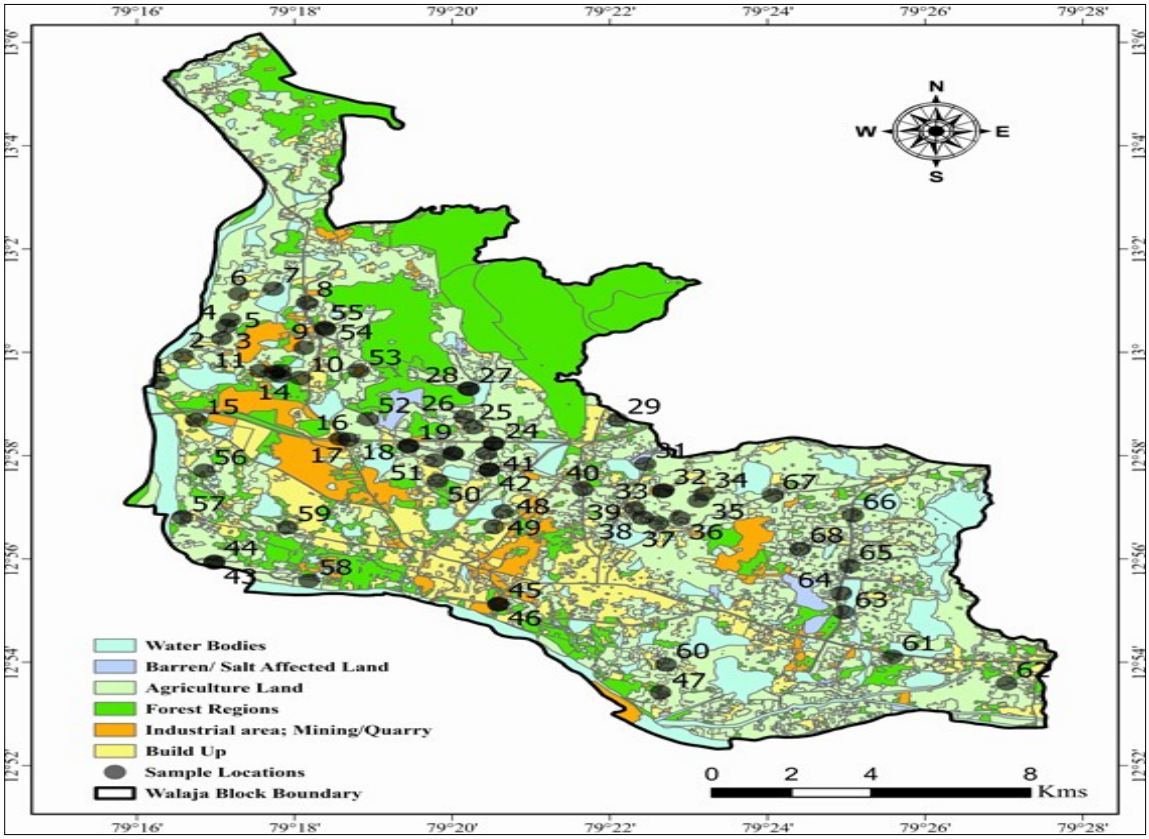

Fig. 1. Study area map showing sampling sites.

Table 1. Indices used for soil contamination assessment with their formulas, classification criteria and interpretations

Name of index	Formula	Classification (values)	Inference	References
Contamination factor (CF)	$CF = C_i / C_n$	CF < 1	Low contamination	(21, 22)
		1 ≤ CF < 3	Moderate contamination	
		3 ≤ CF < 6	Considerable contamination	
		CF ≥ 6	Very high contamination	
Geo-accumulation index (Igeo)	$Igeo = \log_2 [C_i / (1.5 \times C_n)]$	Igeo ≤ 0	Class 0 (uncontaminated)	(23)
		0 < Igeo ≤ 1	Class 1 (uncontaminated to moderately contaminated)	
		1 < Igeo ≤ 2	Class 2 (moderately contaminated)	
		2 < Igeo ≤ 3	Class 3 (moderately to strongly contaminated)	
		3 < Igeo ≤ 4	Class 4 (strongly contaminated)	
		4 < Igeo ≤ 5	Class 5 (strongly to extremely contaminated)	
		Igeo > 5	Class 6 (extremely contaminated)	
Potential ecological risk (Er) - single metal	$Er = T_r \times (C_i / C_n)$	Er < 40	Low risk	(24)
		40 ≤ Er < 80	Moderate risk	
		80 ≤ Er < 160	Considerable (or "significant") risk	
		160 ≤ Er < 320	High risk	
		Er ≥ 320	Very high risk	

(CF - Contamination factor, Igeo - Geo-accumulation index, Er - Potential ecological risk, C_i - Measured concentration of element, C_n - Background/reference value/concentration of element (100 mg kg^{-1} for Cr), T_r -Toxic-response factor (commonly used: T_r (Cr) = 2))

Classification schemes for CF, Igeo and Er are shown in Table 1.

Geostatistical analysis

Spatial interpolation of Cr concentrations and indices (CF, Igeo, Er) was conducted using the inverse distance weighting (IDW) method in QGIS 3.28. Inverse distance weighting estimates values at unsampled locations as weighted averages of nearby observations, with weights declining as the square of distance. A power value of 2 was used, with a fixed search radius including 10 -12 nearest neighbours and a 100 m output grid resolution. Inverse distance weighting was chosen because it is effective for moderate sample sizes and is commonly applied in soil heavy metal mapping (4, 26).

Hotspot analysis

Hotspots of Cr were identified using the Getis–Ord Gi* statistic, which detects statistically significant clusters of unusually high or low values by comparing local sums to global averages (27). For each sampling location, a Z-score and *p*-value were calculated, with significance assessed at the 90 % (|Z| ≥ 1.65), 95 % (|Z| ≥ 1.96) and 99 % (|Z| ≥ 2.58) confidence levels. We performed the analysis using the hotspot analysis (Getis–Ord Gi*) tool in QGIS (processing toolbox → vector analysis), which generated maps of Cr hotspots (high positive |Z| -scores) and cold spots (low negative |Z| -scores). Similar applications in soil contamination mapping have demonstrated the utility of Gi* for detecting local clusters (4).

Risk zonation

Individual index maps (Cr, CF, Igeo, Er) were reclassified into ordinal classes (e.g., low to high) based on their classification schemes. These layers were integrated using a weighted overlay analysis in QGIS. The Er was assigned the highest weight due to its direct ecological relevance, followed by CF and Igeo and then the raw Cr concentration (percentile-based). In weighted overlay, each cell's standardized score is multiplied by its assigned weight

and the results are summed to produce a composite risk surface. The composite raster was then reclassified into three categories: low, moderate and high risk. Weighted overlay methods have been widely used in geographic information system (GIS)-based environmental risk assessments (28).

Correlation analysis

Pearson correlation analysis was performed to examine relationships between soil Cr concentrations and soil properties (pH, EC, SOC). Correlation coefficients (r) and significance levels ($p < 0.05$) were calculated using R software (v4.4). Pearson correlation is widely employed in soil heavy metal studies to infer controlling factors and potential contaminant sources (26).

Results and Discussion

Descriptive statistics

Soil property measurement revealed neutral to slightly alkaline conditions across Walaja block (Table 2), with pH values ranging from 6.10 to 8.86 (mean ≈ 7.34), typical of alluvial soils in semi-arid South India, which often foster Cr(III) precipitation under such pH (29). Electrical conductivity varied between 0.04 and 0.66 dS m^{-1} (mean ≈ 0.255), indicating generally low to moderate salinity, while SOC spanned 0.27 to 3.98 % (mean ≈ 1.05 %), showing low fertility overall with localized organic enrichment. Total Cr concentrations were extremely elevated, ranging from 129 to 2,625 mg/kg with a mean of approximately 601.08 mg/kg, exceeding natural crustal or typical background values (≈ 80–100 mg/kg Cr in many uncontaminated soils) (25) by more than an order of magnitude in many places, signaling strong anthropogenic contamination possibly from tannery and associated industrial effluent (30, 31). The spatial distribution patterns of soil pH, EC, SOC and Cr across the study area are presented in Fig. 2–5.

Pollution and ecological risk indices

The CF values ranged from 1.29 to 26.25 (mean = 14.87), well above the very high contamination threshold (CF > 6) defined by previously (24). The Igeo values ranged from –0.22 to 4.13 (mean = 3.00), placing most sites in the strongly polluted category, with a few approaching the very strongly polluted level (23). Similar Igeo ranges (2.0–4.5) have been reported in soils near tannery clusters in Kenya and Pakistan (30, 32). The Er values ranged from 2.58 to 52.5 (mean = 29.7), remaining largely in the low-risk class (Er < 40), with only a few samples reaching the moderate risk range (40–80). This pattern reflects the relatively low toxic-response factor for Cr ($T_r = 2$) (24). Overall, the CF and Igeo values indicate severe contamination in many locations. For context, similar Igeo ranges (≈2.0–4.5) have been observed in tannery-impacted soils elsewhere (30, 32). The relatively low Er values reflect chromium's lower toxicity weight (24), but all indices agree on the spatial pattern described below.

Correlation analysis

Pearson correlations (Fig. 6) show Cr concentration is perfectly correlated with CF and Er (r=1.00 by definition) and strongly with Igeo ($r = 0.93$). Soil pH exhibited a weak negative correlation with Cr ($r \approx -0.16$). Electrical conductivity correlated moderately negatively with Cr ($r \approx -0.39$), while SOC was weakly positive ($r \approx +0.13$). These patterns suggest that higher pH tends to slightly reduce Cr retention (24), consistent with alkaline soils favoring mobile chromate species. Under alkaline conditions, Cr exists mainly as soluble chromate ($CrO_4^{2-}/Cr_2O_7^{2-}$) (33–35), while protonation of mineral surfaces at lower pH enhances Cr adsorption (36, 37). The observed negative EC–Cr correlation differs from some studies (38), possibly because local salinity is dominated by NaCl from irrigation, which competes with chromate for adsorption sites and increases ionic strength, promoting Cr desorption and leaching (39). The weak positive SOC–Cr correlation is consistent with organic matter's role in binding metals (40, 41). In summary, aside from the expected direct dependence on Cr itself (as seen in CF/Igeo/Er), soil chemical properties seem to play only minor roles in Cr distribution here.

Spatial distribution of Cr and index values

Inverse distance weighted mapping reveals a distinct spatial pattern of Cr contamination (Fig. 7-9). The highest Cr concentrations and worst index values are tightly co-located in the northwestern industrial/tannery corridor (Ranipet, Manthangal, Vanapadi, Walajapet and Ammoor). In these zones many points have Igeo >3 (strongly polluted) and CF >10, indicating very severe pollution. This pattern is consistent with point-source loading from local industry; for example, previous work linked Ranipet's high soil Cr to the Tamil Nadu Chromate and Chemicals Limited (TCCL) tannery plant (42). By contrast, the southern agricultural periphery shows substantially lower Cr levels and index classes. Only smaller, less severe elevated patches appear in peri-urban transition zones (such as Anandhalai and Vannivedu), likely reflecting runoff or historic waste transport. These spatial results confirm that Cr contamination is concentrated near the leather-chemical industrial cluster, whereas rural farmland areas remain largely uncontaminated (aside from minor diffuse inputs).

Hotspot analysis

Getis–Ord Gi* hotspot analysis (Fig. 10) statistically confirms the clustering of Cr in the industrial region. Two sites in the northwestern/tannery belt are significant hotspots (Gi* $|Z| \approx +2.20, p \approx 0.027$) at the 95 % confidence level; these sites (Cr ≈1,538–1,846 mg/kg) are adjacent near the Ranipet–Manthangal/Vanapadi area (27, 43). In other words, each hotspot location has both high Cr and neighbors with high Cr, yielding large positive

Table 2. Descriptive statistics for soil parameters (pH, EC, SOC, Cr) and contamination indices (CF, Igeo, Er)

Variable	Mean	Median	SD	Min	Max	Skewness	Kurtosis
pH	7.34	7.30	0.66	6.10	8.86	0.18	-0.71
EC	0.26	0.26	0.15	0.04	0.66	0.61	-0.18
SOC	1.05	0.71	0.73	0.27	3.98	1.66	3.25
Cr	601.08	372	612.47	128.75	2625.00	2.22	4.33
CF	14.87	16.23	7.25	1.29	26.25	-0.39	-0.88
Igeo	3.00	3.44	1.14	-0.22	4.13	-1.50	1.40
Er	29.74	32.47	14.49	2.58	52.50	-0.39	-0.88

EC - Electrical conductivity, SOC - Soil organic carbon, Cr – Chromium, CF - Contamination factor, Igeo – Geo accumulation index, Er - Potential ecological risk, SD – Standard deviation, Min – Minimum, Max – Maximum

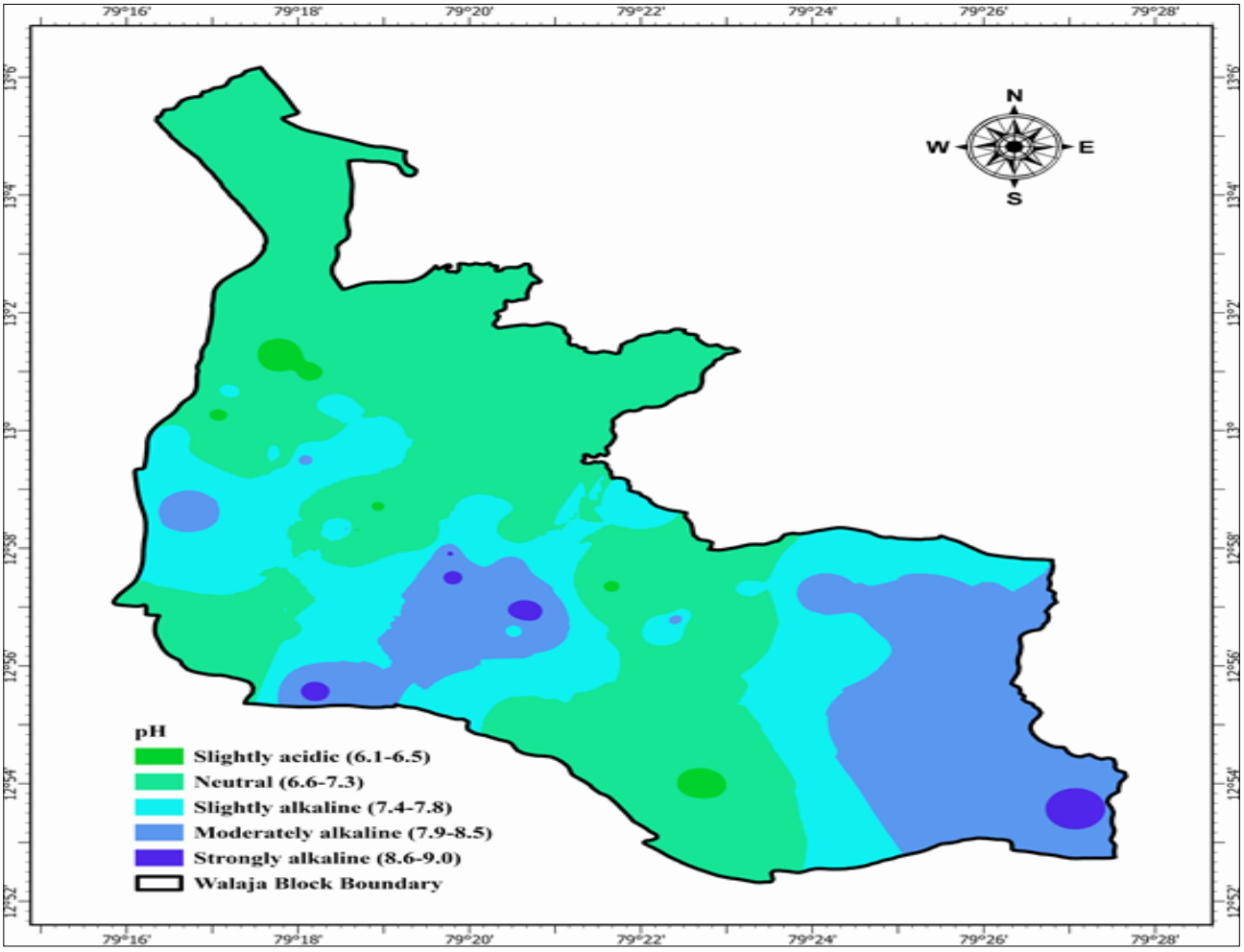

Fig. 2. Spatial distribution of soil pH across the study area.

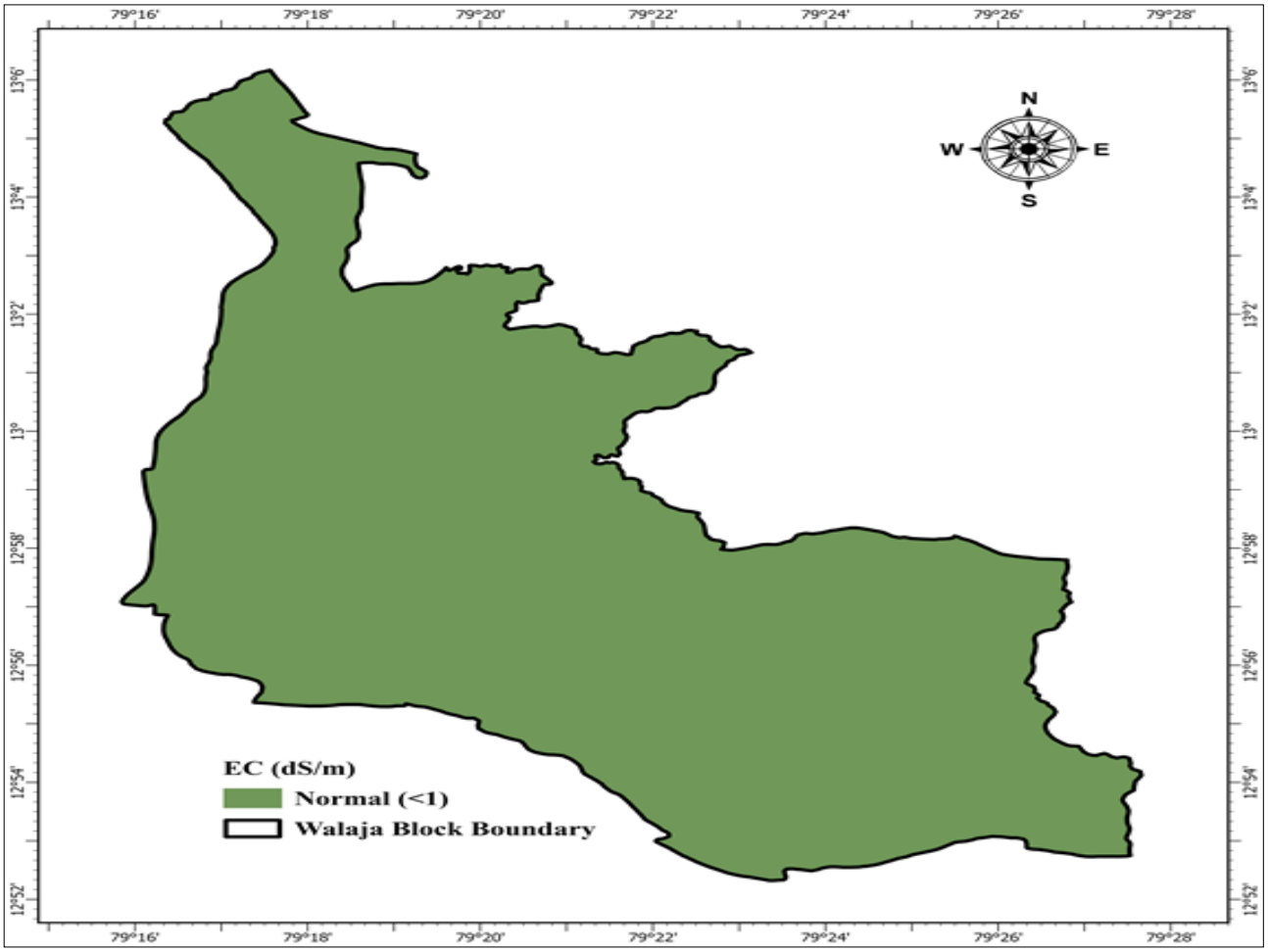

Fig. 3. Spatial distribution of SOC.

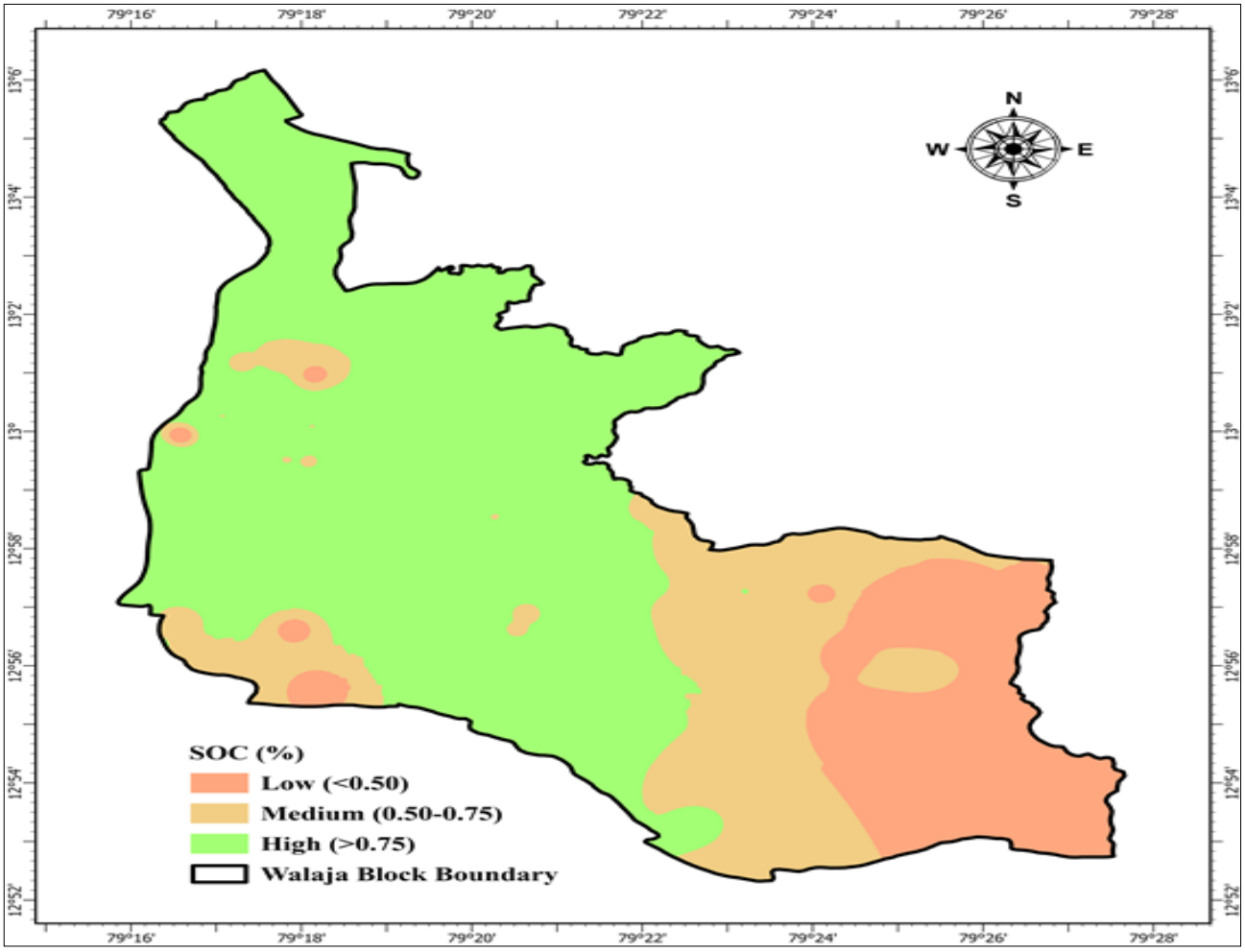

Fig. 4. Spatial distribution of SOC.

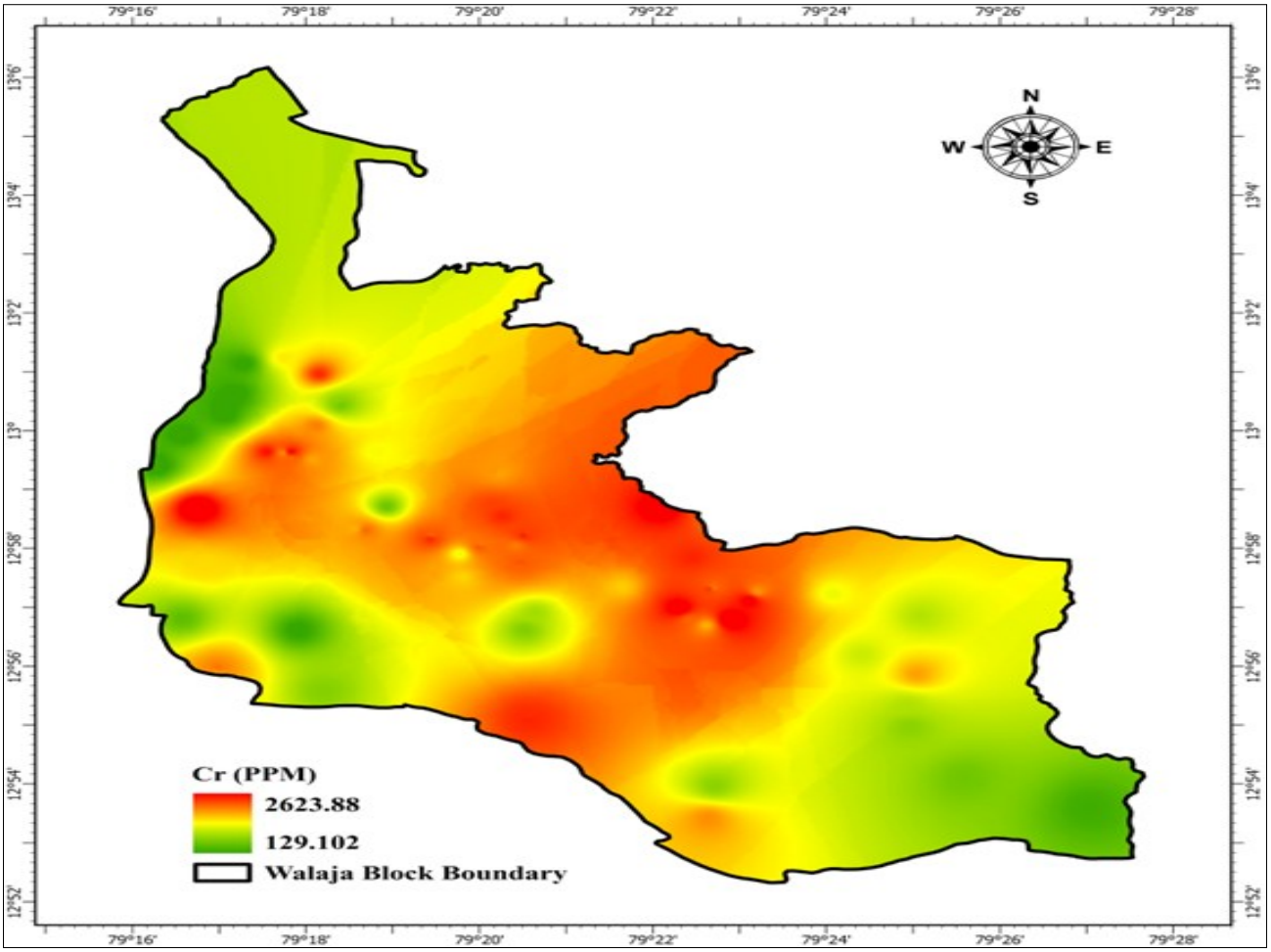

Fig. 5. Spatial distribution of Cr concentration in soils.

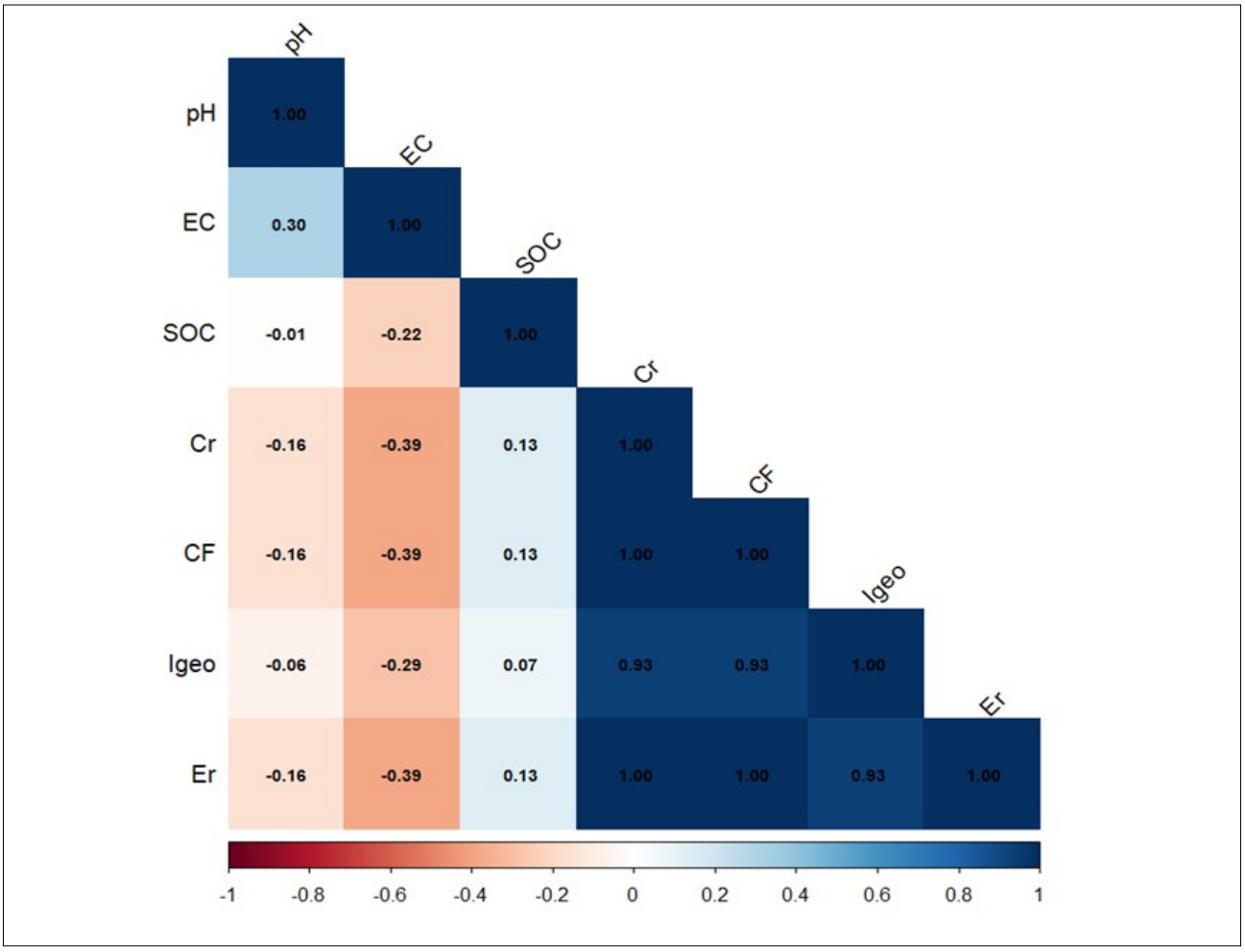

Fig. 6. Correlation matrix heat map of soil properties and pollution indices.

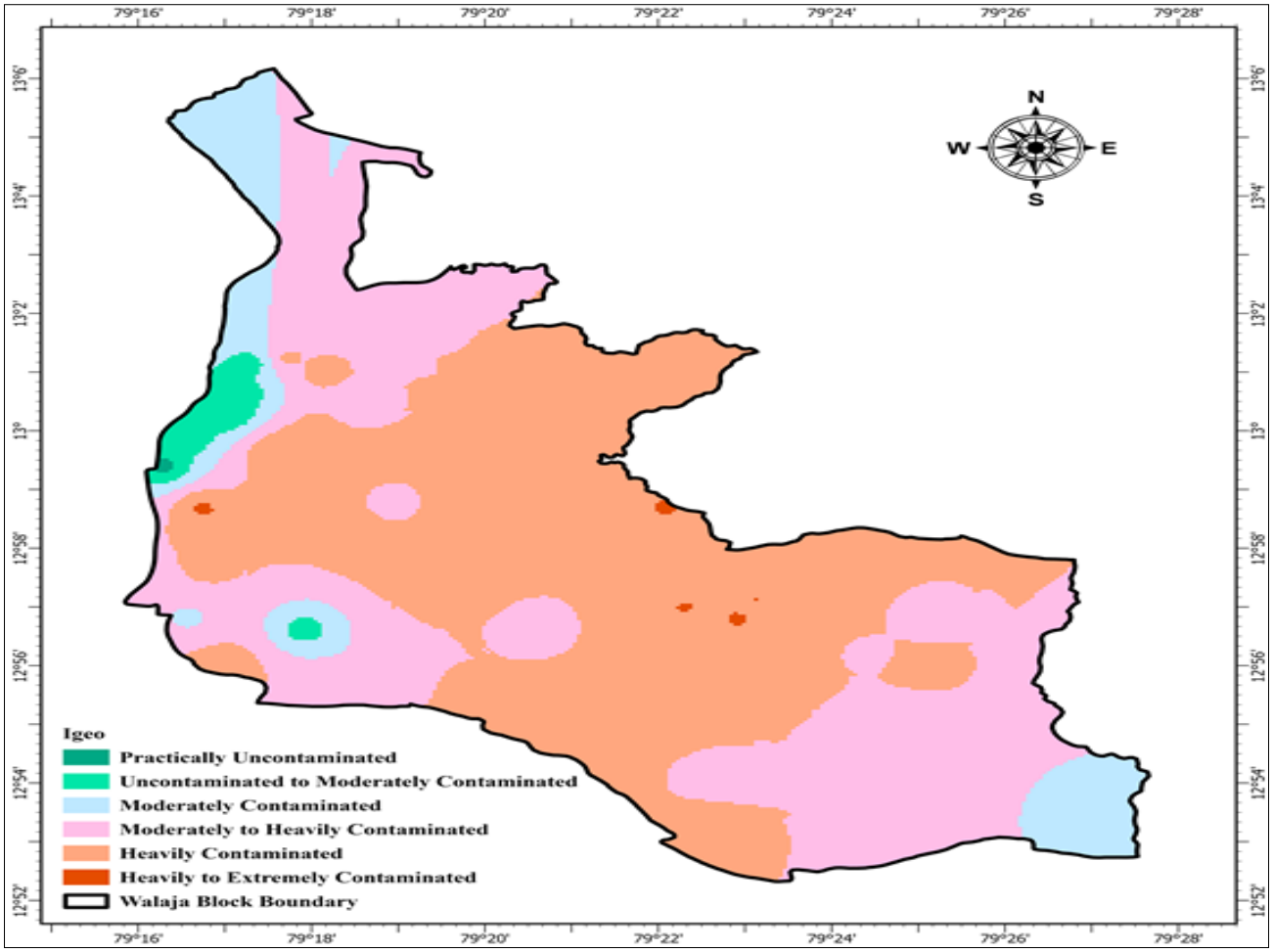

Fig. 7. Spatial distribution of the Igeo.

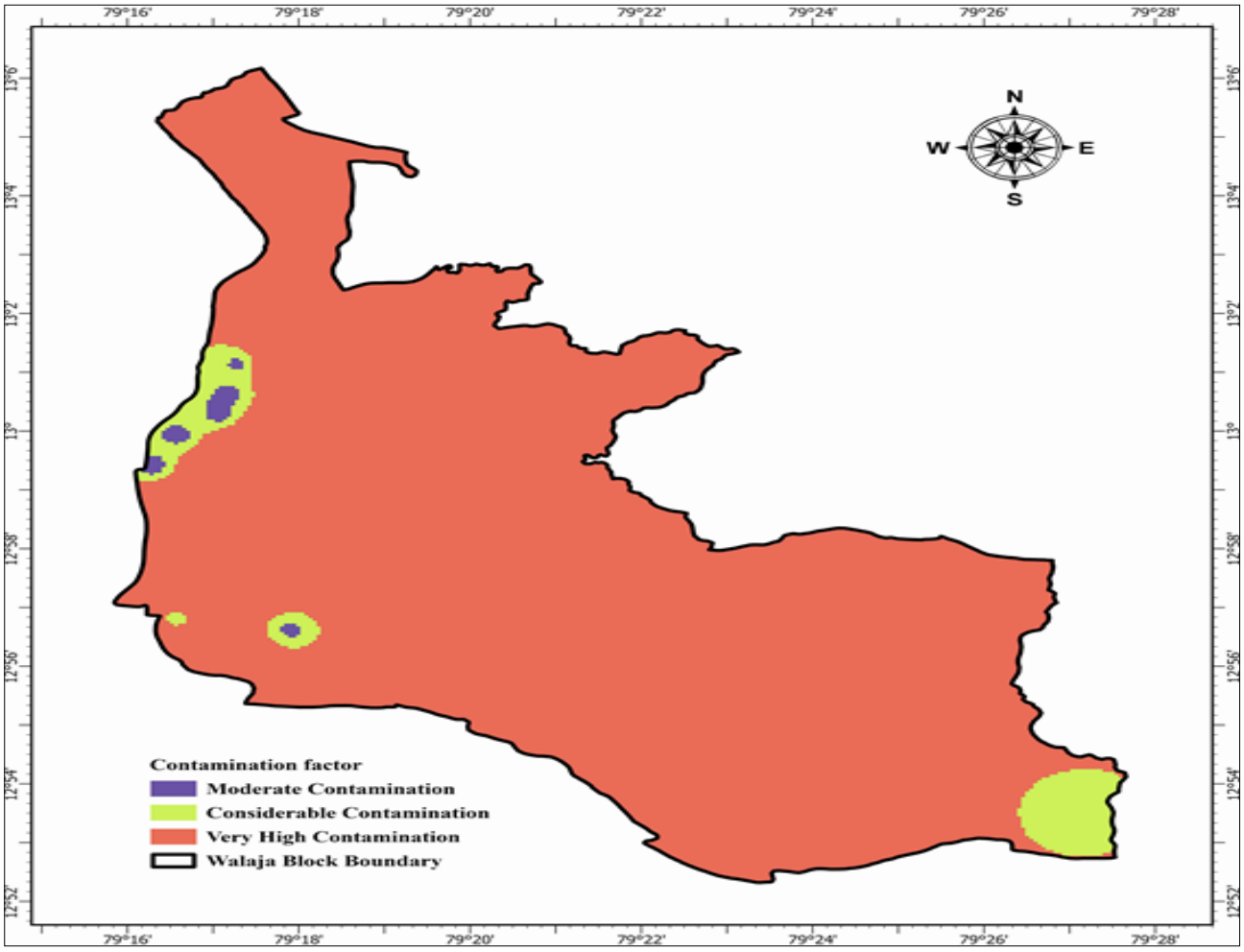

Fig. 8. Spatial distribution of the CF.

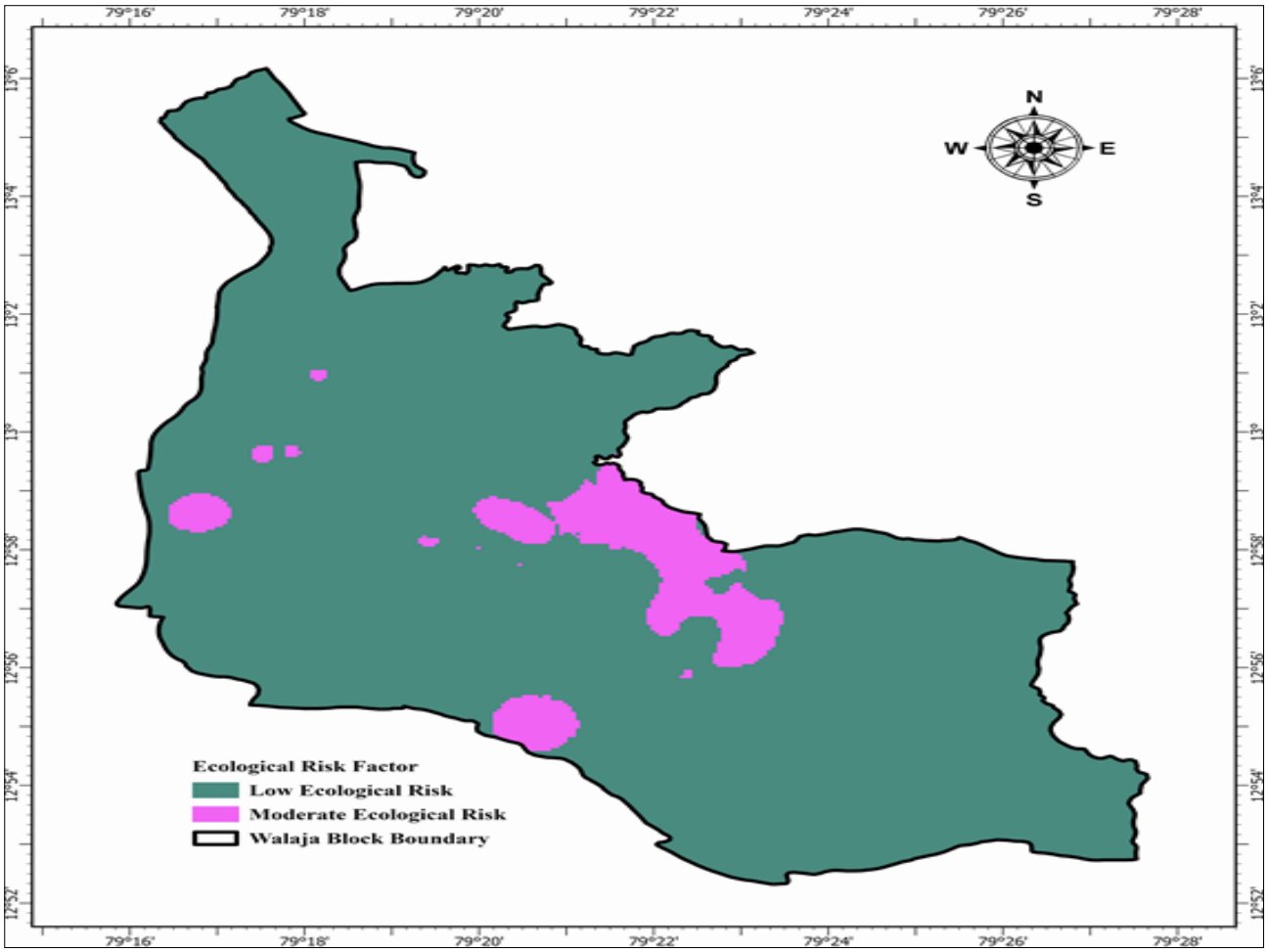

Fig. 9. Spatial distribution of the potential Er.

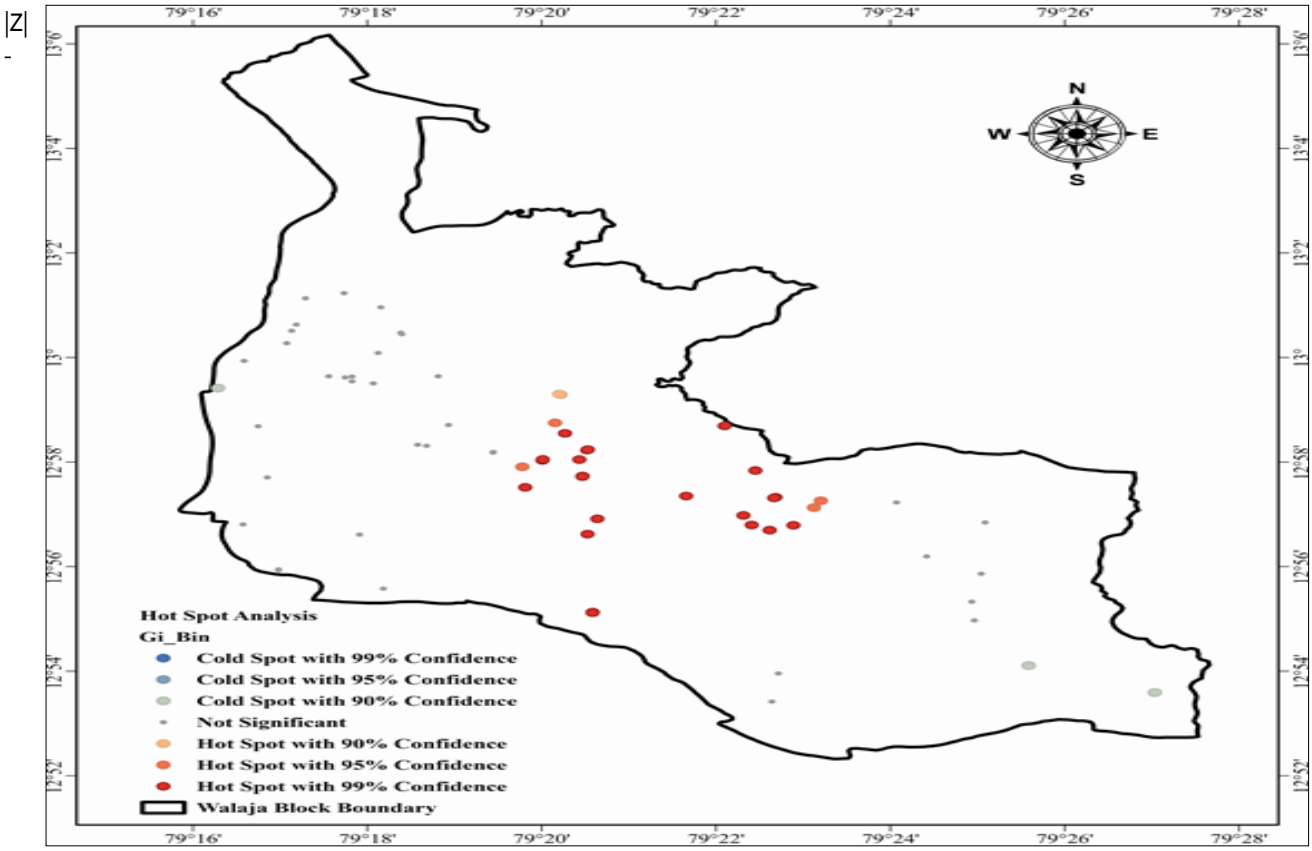

Fig. 10. Spatial delineation of potential ecological risk zones based on CF, Igeo, Er and Cr level classes.

scores. Conversely, three locations in the southern/eastern rural periphery are significant coldspots (Gi* |Z| ≈ –2.10 to –2.17, p<0.05) with much lower Cr (≈129–637 mg/kg) surrounded by similarly low values. These results reinforce the land-use contrast: the industrial/tannery corridor (Ranipet, Ammoor) is anomalously Cr-rich, while the agrarian outskirts are statistically low in Cr. For example, sampling sites south of Walajapet (near Vannivedu) fall in the 95 % confidence coldspot category, reflecting uniformly low contamination. While irrigation runoff, ploughing and percolation may dilute and redistribute Cr in agricultural zones, all topsoil samples south of Walajapet still exceed FAO limits, showing that such processes have not reduced surface concentrations to safe levels. Overall, hotspot analysis shows that high-Cr clusters coincide with known tannery zones, supporting the conclusion that leather and chemical industries are the primary Cr sources.

Integrated risk zonation

Using the index maps of CF, Igeo, Er and Cr concentration, pollution levels were reclassified and integrated to derive overall risk categories (low, moderate and high) (Fig. 11). The integration employed a weighted linear combination approach, assigning weights of 0.4, 0.2, 0.2 and 0.2 to CF, Igeo, Er and Cr, respectively, to reflect their relative contributions to contamination intensity and ecological hazard. The resulting risk zonation map indicates that approximately 20 % of the area falls under high-risk zones, forming a continuous belt coincident with the industrial and tannery cluster; about 35–40 % of the area corresponds to moderate-risk zones, predominantly within mixed land-use transition zones; and the remaining 40–45 % represents low-risk areas, largely associated with agricultural fields and rural settlements. Notably, some administrative village units contain embedded high-risk pixels, suggesting that aggregated boundary analyses may obscure finer-scale heterogeneity. The spatial pattern of risk aligns closely with results from IDW interpolation and Getis-Ord Gi* analyses, reaffirming that chromium contamination and associated ecological risks are concentrated within the industrial corridor (44, 45).

Influence of land use and contamination sources

All spatial analyses (distribution maps of Cr, Igeo, CF, Er, hotspot analysis and risk zonation) reflect local land use. Industrial/tannery areas (the Ranipet/Walajapet belt) correspond exactly to the high index values and Gi* hotspots, reflecting intense point-source loading. Tanneries, plating shops and other factories lie along the Palar River basin, discharging untreated effluent that floods into surrounding fields during rains. Communities along the Palar River bear the toxic cost of untreated tannery waste, with Supreme Court authorities noting irreversible damage to water bodies, groundwater and agricultural lands (46). This explains why peri-urban downriver sites (e.g. Vannivedu, Anandhalai) show moderately elevated Cr – they likely receive washed-in contaminants from upstream. In contrast, purely agricultural southern villages lack such industries and appear as Gi* coldspots with uniformly low Cr. In short, the maps and indices consistently highlight leather-chemical industrial zones as the Cr sources, whereas rural farmland areas are largely uncontaminated (apart from minor diffuse effects).

Across all measures, the industrial belt emerges as the center of pollution. Minor differences among indices stem from their definitions (e.g. Er uses a low toxicity factor for Cr (24), whereas CF and Igeo scale directly with concentration), but every method identifies the same clusters. The Getis–Ord Gi* analysis statistically confirms the spatial clusters seen in the CF and Igeo maps and the integrated risk map fuses these perspectives. These findings align with other studies of tannery regions (30,

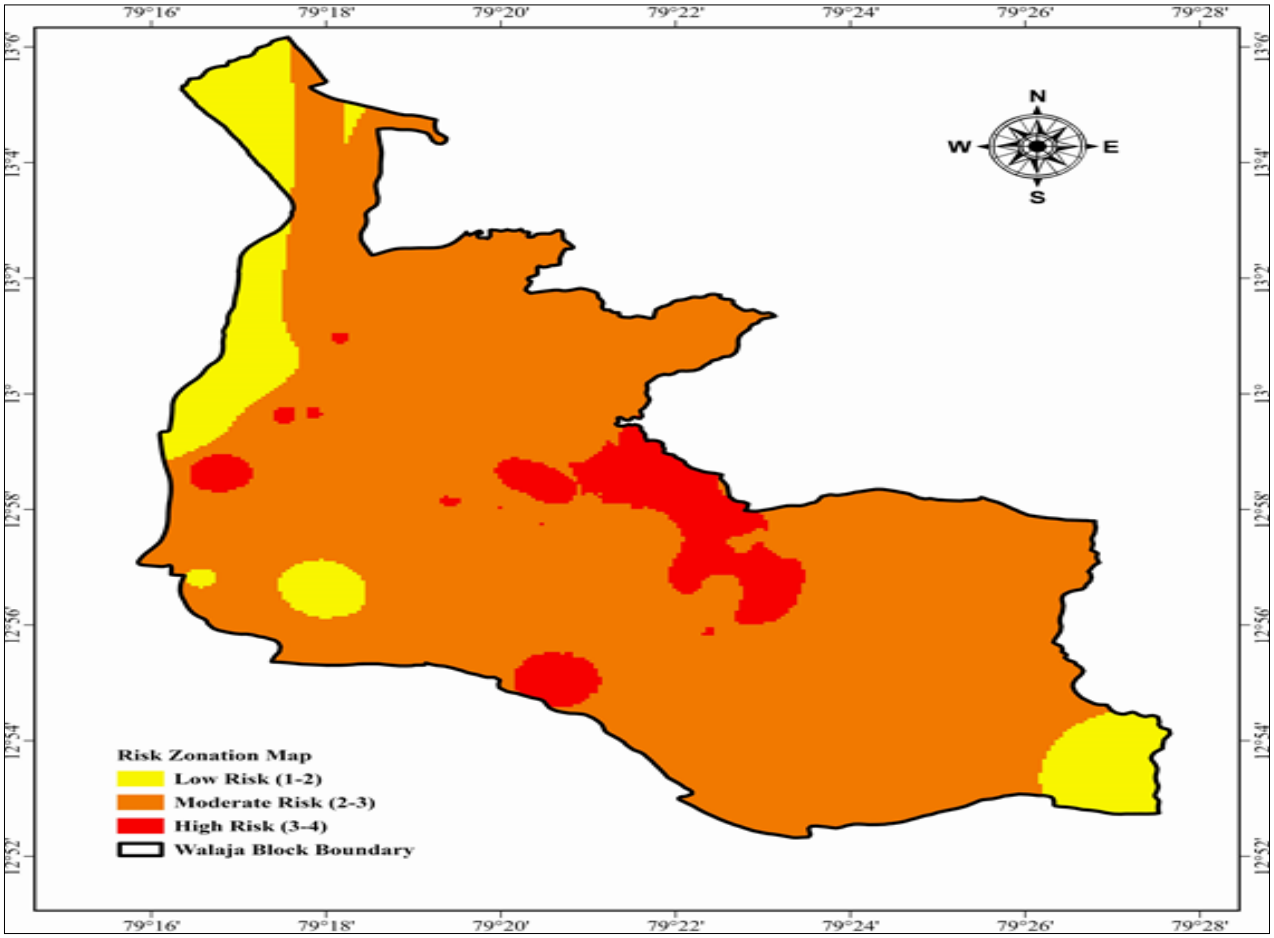

Fig. 11. Spatial delineation of potential ecological risk zones based on CF, Igeo, Er and Cr level classes.

38), where effluent discharge produces sharp Cr gradients and hotspots around factory areas. In summary, high-risk zones coincide with industrial land use and effluent pathways, while low-risk zones align with agricultural land. This consistency across indices reinforces confidence in our results and underscores that anthropogenic sources dominate the spatial risk profile of Cr in Walaja block.

Conclusion

Chromium contamination in Walaja block is predominantly concentrated in the Ranipet–Walajapet leather/chemical belt, with clear hotspot clusters in Ranipet, Manthangal and Vanapadi and markedly lower levels observed in the distant agricultural zones. Multiple spatial indices and risk metrics consistently converge on this spatial pattern and the distribution closely correlates with local land use and drainage. Tannery and industrial discharges along the Palar River are the primary drivers of downstream soil Cr accumulation. Although geochemical indices classify contamination as extreme in the hotspot corridor, the overall ecological-risk score is moderate because of Cr's toxicity weighting; nonetheless the human and agricultural exposure potential in hotspot areas is high. Approximately one-fifth of the study area (the northwestern industrial belt) falls into a high-risk class, with another ≈35–40 % in moderate-risk transition zones-these should be the priority for intervention and monitoring.

Practical actions are clear: (i) prioritize containment and remediation at tannery effluent lines, industrial parcels and adjacent fields; (ii) retrofit or enforce effluent treatment and waste management at tanneries; (iii) implement frequent soil monitoring in identified hotspots and along drainage paths; and (iv) evaluate on-site mitigation such as soil amendments to reduce Cr mobility. This integrated spatial approach provides a robust ad reproducible framework for risk zoning in industrial watersheds and offers actionable insights for policymakers and local authorities to effectively target remediation efforts and safeguard agricultural productivity and public health.

Acknowledgements

The authors are grateful to Centre for Water & Geospatial Studies, Tamil Nadu Agricultural University, Coimbatore, for providing lab and financial support through TNPCB project. The authors immensely delighted to convey their deepest and heartfelt thank to the Department of Remote Sensing & GIS, Tamil Nadu Agricultural University.

Authors' contributions

All the authors contributed equally to the conceptualisation of the work, interpretation, analysis, writing, reviewing and editing of the manuscript. All authors read and approved the final manuscript.

Compliance with ethical standards

Conflict of interest: Authors do not have any conflict of interest to declare.

Ethical issues: None

Declaration of generative AI and AI-assisted technologies in the writing process: During the preparation of this work, the authors used ChatGPT (OpenAI) and Springer's language editing services to enhance clarity and readability. After using these tools, the authors reviewed and edited the content as needed and take full responsibility for the publication's content.

References

1. Food and Agriculture Organization of the United Nations (FAO). The state of the world's land and water resources for food and agriculture 2022 – Systems at breaking point. Rome: FAO; 2022. https://doi.org/10.4060/cb9910en
2. Hou D, Jia X, Wang L, McGrath SP, Zhu YG, Hu Q, et al. Global soil pollution by toxic metals threatens agriculture and human health. Science. 2025;388(6744):316–21. https://doi.org/10.1126/science.adr5214
3. Jaishankar M, Tseten T, Anbalagan N, Mathew BB, Beeregowda KN. Toxicity, mechanism and health effects of some heavy metals. Interdiscip Toxicol. 2014;7(2):60. https://doi.org/10.2478/intox-2014-0009
4. Huo XN, Li H, Sun DF, Zhou LD, Li BG. Combining geostatistics with Moran's I analysis for mapping soil heavy metals in Beijing, China. Int J Environ Res Public Health. 2012;9(3):995–1017. https://doi.org/10.3390/ijerph9030995
5. Huang C, Gou Z, Ma X, Liao G, Deng O, Yang Y. Quantification of sources and potential risks of cadmium, chromium, lead, mercury and arsenic in agricultural soils in a rapidly urbanizing region of southwest China: The case of Chengdu. Front Public Health. 2024;12:1400921. https://doi.org/10.3389/fpubh.2024.1400921
6. International Agency for Research on Cancer (IARC). IARC monographs on the evaluation of carcinogenic risks to humans. Vol. 100D: Radiation. Lyon: IARC; 2012.
7. Ratnalu GV, Dhakate R, More S. Distribution and human health hazard appraisal with special reference to chromium in soils from Peenya industrial area, Bengaluru City, South India. J Environ Health Sci Eng. 2022;20(1):79–100. https://doi.org/10.1007/s40201-021-00757-z
8. Islam MM, Rahman T, Urmi AAZ, Mamun MIR, Shoeb M. Impact of the tannery industrial zone on physicochemical and microbiological quality of Dhaleshwari river water, Bangladesh. J Bangladesh Acad Sci. 2025;49(1):45–55. https://doi.org/10.3329/jbas.v49i1.75146
9. Ambiga K, Annadurai R, Vinayagamoorthy R. Nitrate and chromium contamination in groundwater from effluent of tanneries and drastic vulnerability index map: A case study of Ranipet area, Vellore district, Tamilnadu. Indian J Sci Technol. 2016;9:40. https://doi.org/10.17485/ijst/2016/v9i40/92439
10. Murugaiyan S, Velusamy S, Maheswari M, Dhevagi P, Kalpana P, Dinesh GK, Prasad S, Shivprasad. Evaluation and speciation of heavy metals in the soil of the suburban region of Southern India. Soil Sediment Contam. 2022;31(6):520–39.
11. Sinduja M, Sathya V, Maheswari M, Dhevagi P, Sivakumar U, Chitdeshwari T, et al. Chromium speciation and agricultural soil contamination in the surrounding tannery regions of Walajaphet, Vellore district, Southern India. Madras Agric J. 2022;3(1–3):1. https://doi.org/10.1080/15320383.2022.2030298
12. Anna university, centre for climate change and disaster management. Ranipet district profile. Chennai: Anna University; 2023. https://www.annauniv.edu/cccdm/districtprofiles/ranipet.html
13. Arivoli S, Vassou M, Tennyson S, Meeran M, Ramanan A, Divya S, Kamatchi P. Analysis of soil and water quality in selected villages of Ranipet district, Tamil Nadu, India. Magnesium. 2021;200:200. http://dx.doi.org/10.12944/CWE.16.2.14
14. Central Ground Water Board (CGWB). Groundwater yearbook of Tamil Nadu and U.T. of Puducherry (2018–2019). 2019.
15. Marius K, Venkatasubramanian G. Exploring urban economic resilience: The case of a leather industrial cluster in Tamil Nadu. Savoirs et Mondes Indiens Working Papers Series. 2017. https://doi.org/10.3917/ried.236.0137
16. Soil science division staff. Soil survey manual. Washington (DC): USDA, Natural Resources Conservation Service; 2017. p. 603. (USDA Handbook No. 18). Minor amendments 2018.
17. American public health association (APHA). Standard methods for the examination of water and wastewater. 23rd ed. Washington (DC): APHA; 2017. https://www.standardmethods.org/
18. Jackson ML. Soil chemical analysis. New Delhi: Prentice Hall of India Pvt Ltd; 1973.
19. Walkley A, Black IA. An examination of the Degtjareff method for determining soil organic matter and a proposed modification of the chromic acid titration method. Soil Sci. 1934;37(1):29–38. https://doi.org/10.1097/00010694-193401000-00003
20. US Environmental Protection Agency. Method 3051a- microwave assisted acid digestion of sediments, sludges, soils and oils; 1998.
21. Ahamad MI, Song J, Sun H, Wang X, Mehmood MS, Sajid M, et al. Contamination level, ecological risk and source identification of heavy metals in the hyporheic zone of the Weihe River, China. Int J Environ Res Public Health. 2020;17(3):1070. https://doi.org/10.3390/ijerph17031070
22. Ni J, Yuan C, Zheng J, Liu Y. Distributions, contamination level and ecological risk of heavy metals in surface sediments from intertidal zone of the Sanmen Bay, East China. J Sea Res. 2022;190:102302. https://doi.org/10.1016/j.seares.2022.102302
23. Muller G. Index of geo-accumulation in sediments of the Rhine River. 1969.
24. Hakanson L. An ecological risk index for aquatic pollution control. Water Res. 1980;14(8):975–1001. https://doi.org/10.1016/0043-1354(80)90143-8
25. Turekian KK, Wedepohl KH. Distribution of the elements in some major units of the Earth's crust. Geol Soc Am Bull. 1961;72(2):175–92. https://doi.org/10.1130/0016-7606(1961)72
26. Sun L, Guo D, Liu K, Meng H, Zheng Y, Yuan F, Zhu G. Levels, sources and spatial distribution of heavy metals in soils from a typical coal industrial city of Tangshan, China. Catena. 2019;175:101–9. https://doi.org/10.1016/j.catena.2018.12.014
27. Getis A, Ord JK. The analysis of spatial association by use of distance statistics. Geogr Anal. 1992;24(3):189–206. https://doi.org/10.1111/j.1538-4632.1992.tb00261.x
28. Zhang C, Luo L, Xu W, Ledwith V. Use of local Moran's I and GIS to identify pollution hotspots of Pb in urban soils of Galway, Ireland. Sci Total Environ. 2016;556:1–10. https://doi.org/10.1016/j.scitotenv.2016.02.166
29. Kabata-Pendias, Alina. Trace elements in soils and plants. 3rd ed. Boca Raton (FL): CRC Press; 2000. https://doi.org/10.1201/9781420039900
30. Oruko RO, Edokpayi JN, Msagati TA, Tavengwa NT, Ogola HJ, Ijoma G, et al. Investigating chromium status, heavy metal contamination and ecological risk assessment via tannery waste disposal in sub-Saharan Africa (Kenya and South Africa). Environ Sci Pollut Res. 2021;28(31):42135–49. https://doi.org/10.1007/s11356-021-13703-1
31. Zulfiqar U, Haider FU, Ahmad M, Hussain S, Maqsood MF, Ishfaq M, et al. Chromium toxicity, speciation and remediation strategies in soil-plant interface: A critical review. Front Plant Sci. 2023;13:1081624. https://doi.org/10.3389/fpls.2022.1081624
32. Eze O, Tukura B, Atolaiye B, Opaluwa O. Index model assessment of heavy metal pollution in soils selected from three irrigated farm sites in Abuja, Nigeria. Int J Adv Sci Res Eng. 2018;4(6):93–105. https://doi.org/10.31695/IJASRE.2018.32758
33. McBride MB. Environmental chemistry of soils. New York: Oxford

University Press; 1994.

34. Sparks DL. Environmental soil chemistry. 2nd ed. San Diego (CA): Academic Press; 2003. https://doi.org/10.1016/B978-012656446-4/50001-3

35. Kabata-Pendias A. Trace elements in soils and plants. 4th ed. Boca Raton (FL): CRC Press; 2010. https://doi.org/10.1201/b10158

36. Rinklebe J, Shaheen SM. Redox chemistry of chromium in soils and sediments. Chemosphere. 2017;613–14:1140–52. https://doi.org/10.1016/j.chemosphere.2017.02.153

37. Lee SZ, Chang L, Ehrlich RS. The relationship between adsorption of Cr(VI) and soil properties. J Environ Sci Health, Part A. 1999:34 (4):809–33. https://doi.org/10.1080/10934529909376867

38. Ali Z, Malik R, Shinwari Z, Qadir A. Enrichment, risk assessment and statistical apportionment of heavy metals in tannery-affected areas. Int J Environ Sci Technol. 2015;12(2):537–50. https://doi.org/10.1007/s13762-013-0428-4

39. Dhal B, Thatoi HN, Das NN, Pandey BD. Chemical and microbial remediation of hexavalent chromium from contaminated soil and groundwater. Chemosphere. 2019;230:366–85. https://doi.org/10.1016/j.jhazmat.2013.01.048

40. Xiao W, Zhang Y, Li T, Chen B, Wang H, He Z, et al. Reduction kinetics of hexavalent chromium in soils and its correlation with soil properties. J Environ Qual. 2012;41(5):1452–58. https://doi.org/10.2134/jeq2012.0061

41. Violante A, Cozzolino V, Perelomov L, Caporale AG, Pigna M. Mobility and bioavailability of heavy metals and metalloids in soil environments. J Soil Sci Plant Nutr. 2010;10(3):268–92. https://doi.org/10.4067/S0718-95162010000100005

42. Veluprabakaran V, Kavitha M. Evaluation of heavy metals in ground and surface water in Ranipet, India utilizing HPI model. Environ Monit Assess. 2023;195(7):875. https://doi.org/10.1007/s10661-023-11452-x

43. Kim SM, Choi Y. Assessment of lead and zinc contamination in beach sands by hotspot analysis. J Coastal Res. 2019;91(SI):321–5. https://doi.org/10.2112/SI91-065.1

44. Torgalkar V, Mohidin R, Turati S, Torsello V. How India's leather industry is polluting a major river basin. Eco-Business. 2025. https://www.eco-business.com/news/how-indias-leather-industry-is-polluting-a-major-river-basin/

45. Ouabo RE, Sangodoyin AY, Ogundiran MB. Assessment of ordinary kriging and IDW methods for modeling chromium and cadmium soil pollution in e-waste sites in Douala, Cameroon. J Health Pollut. 2020;10(26):200605. https://doi.org/10.5696/2156-9614-10.26.200605

46. Al Hamdani Mo. Spatial analysis of soil heavy metals in Dohuk, North of Iraq (Doctoral dissertation); 2024. http://hdl.handle.net/11513/4089

Additional information

Peer review: Publisher thanks Sectional Editor and the other anonymous reviewers for their contribution to the peer review of this work.

Reprints & permissions information is available at https://horizonepublishing.com/journals/index.php/PST/open_access_policy

Publisher's Note: Horizon e-Publishing Group remains neutral with regard to jurisdictional claims in published maps and institutional affiliations.

Indexing: Plant Science Today, published by Horizon e-Publishing Group, is covered by Scopus, Web of Science, BIOSIS Previews, Clarivate Analytics, NAAS, UGC Care, etc
See https://horizonepublishing.com/journals/index.php/PST/indexing_abstracting

Publisher information: Plant Science Today is published by HORIZON e-Publishing Group with support from Empirion Publishers Private Limited, Thiruvananthapuram, India.